

High Sensitivity and Ultra-High-Quality Factor for an all-Optical Temperature Sensor Based On Photonic Crystal Technology

Kouddad Elhachemi*, Dekkiche Leila and Naoum Rafah

Telecommunication and Digital Signal Processing Laboratory, Faculty of Electrical Engineering, Department of Telecommunications, University Djillali Liabes, Sidi-Bel-Abbes 22000, Algeria

***Corresponding author:** Kouddad Elhachemi, Telecommunication and Digital Signal Processing Laboratory, Faculty of Electrical Engineering, Department of Telecommunications, University Djillali Liabes, Sidi-Bel-Abbes 22000, Algeria **E-mail:** kouddad20@hotmail.fr

Received date: 16-November-2022, Manuscript No. tsnst-22-80037; **Editor assigned:** 18-November-2022, PreQC No. tsnst-22-80037 (PQ); **Reviewed:** 30-November-2022, QC No. tsnst-22-80037 (Q); **Revised:** 12-December-2022, Manuscript No. tsnst-22-80037 (R); **Published:** 20-December-2022 **DOI:** 10.37532/0974-7494.2022.16(6).174

Abstract

In our work, we propose a novel temperature sensor design based on a Two-Dimensional (2D) photonic crystal resonant cavity structure designed to detect and monitor temperature under very harsh environmental conditions from 0°C to 500°C. The sensitivity of the proposed structure is 109.8 pm/°C, an ultra-high quality factor, high transmission efficiency and ultra-compact size. The characteristics of the proposed sensor under different temperatures are simulated using the Plane Wave Expansion (PWE) method and Finite Difference Time Domain (FDTD) method to calculate, respectively, the Photonic Band Gap (PBG) and transmission efficiency. The results obtained show that the wavelength of the resonant cavity increases linearly with increasing temperature. Our sensor is suitable for applications based on nanotechnology.

Keywords: Resonant cavities; Sensitivity; Photonic crystal; PWE method; FDTD method; Quality factor

Introduction

In recent years, Photonic Crystal (PhC) has attracted a lot of attention because of its more important properties for controlling and manipulating light through the crystal. Based on this characteristic, many scientists are finding designs and applications for various optical devices, such as optical decoders, logic gas, sensors etc[1-7].

Due to their several advantages such as bandwidth properties and the flexibility of miniaturization, PhC-based devices are now playing a very important role in new fields such as optical sensing [8].

Recently, optical sensors have attracted the attention of researchers because of their advantage over electronic sensors, which are limited in transferring large data at a very higher speed, which can be solved by all-optical sensors, optical switches, and tunable

Citation: Elhachemi K., Leila D., Rafah N. High Sensitivity and Ultra-High-Quality Factor for an all-Optical Temperature Sensor Based on Photonic Crystal Technology. Nano Tech Nano Sci IndJ.2022;16(6):174

©2022 Trade Science Inc.

filters [9-13]. Optical sensors have been used effectively in many applications to detect various parameters such as pressure, biochemical sensors, gas, electric field, and temperature [14-18]. Temperature measurements are very important and are widely used in the risk control application of the petrochemical industry, automotive industry, avionics, industrial safety, biomedicine, and in many other applications[19-22].

Different optical temperature sensors based on 2D-PhC can be realized by ring resonators and waveguides structure [23,24]. Although nanosensors based on ring resonators offer high normalized transmission efficiency, high sensitivity, and high-quality factor [25]. PhC waveguide-based nano-sensors have a good standardized transmission efficiency but a very low-quality factor [26].

In the present work, we have proposed a new hexagonal nanosensor based on a resonant cavity to detect the temperature in the range of 0°C to 500°C. The proposed temperature sensor has a wide range of applications in the defence, chemical, civil, metal production, semiconductor industry, and other fields. Temperature monitoring is also important for estimating the structural health of the device. The proposed design is more compact and simpler. Also, it offers a very high-quality factor and high sensitivity.

Materials and Methods

Bandgap analysis

In this section, we proposed the initial temperature sensor structure based on 2D PhC, with a hexagonal array of circular silicon pillars whose refractive index is equal to 3.42 suspended in the air. The numbers of the pillars in the x and z directions are respectively 23 and 17 and the ratio between the radius « R » and the lattice constant « a » is 0.3 **FIG. 1(a)**.

In general, we use the PWE method to obtain the photonic bandgap which depends on three major parameters such as the lattice constant, the permittivity of dielectric materials, and the radius of the pillars. As shown in **FIG. 1(b)**, there are three PBG regions for the Transverse Electric (TE) mode. The normalized frequency (a/λ) ranges for the three regions are (0.23-0.32), (0.42-0.54), and (.64-0.75). The second wavelength range of the PBG is between 1481.48 nm and 1904.76 nm, which is suitable for the proposed sensor design because it belongs to the third window of optical telecommunications.

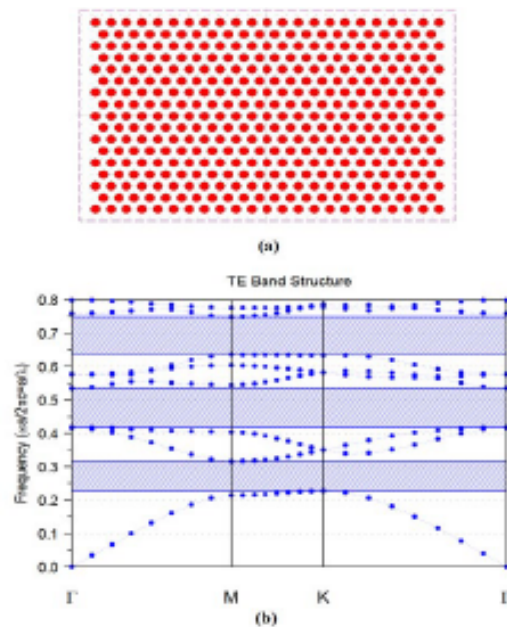


FIG. 1. Initial Structure (a) Pillars in the air (hexagonal lattice) (b) Band gap structure for the TE mode.

Analysis of temperature effects

In our study, using the FDTD method that allows us to calculate the spectral efficiency due to the propagation of the optical field from solving the differential equations of Maxwell in the time domain. Based on these Maxwell's equations, we can calculate the optical field in each position of the space inside the 2D structures based on photonic crystals for the TE mode, written as follows:

$$\frac{\partial E_z}{\partial y} - \mu \frac{\partial H}{\partial t} - \sigma_m H_x \quad (1)$$

$$\frac{\partial E_z}{\partial x} = \mu \frac{\partial H_y}{\partial t} - \sigma_m H_y \quad (2)$$

$$\frac{\partial H_y}{\partial x} - \frac{\partial H_x}{\partial y} = \epsilon \frac{\partial E_z}{\partial t} - \sigma H_z \quad (3)$$

ϵ is the permittivity, σ is the conductivity and μ is the permeability.

To optimize the two-dimensional calculations to the simulation of an optical wave, using the Perfectly Matched Layer (PML) as the boundary conditions of absorption which is defined by the following equation:

$$\Delta t \leq \frac{1}{c \sqrt{\frac{1}{\Delta x^2} + \frac{1}{\Delta y^2}}} \quad (4)$$

Δx and Δy represents the spatial steps in the x and y directions.

c is the speed of light in a vacuum.

The detection operation of an all-optical temperature sensor is based on the refractive index variation as a function of the thermo-optical effect. The refractive index will be modified according to the temperature, which allows the photonic band gap and the centre wavelength of the structure to be changed, and this variation is given as [27]:

$$n = n_0 + \alpha T$$

n_0 is the refractive index of the medium at zero temperature ($0^\circ C$), α is the thermo-optical coefficient given by $2.4 \times 10^{-4}/^\circ C$ for silicon and ΔT is the temperature difference [28].

Results and Discussion

The designed temperature sensor structure of the 2D hexagonal shape based on the resonant cavity is shown in **FIG. 2**. Our sensor is composed of two quasi-waveguides in the horizontal in-line direction, and a resonant cavity is located between them. The in-line quasi-waveguides are created by removing nine silicon pillars for both sides as input and output. The resonant cavity is created by optimizing rays of some internal pillars such as black rods ($R*1.3$), blue rods ($R*0.5$), and green rods ($R*0.45$) placed in the hexagonal array to couple the light signal into quasi-in-line waveguides from the input to the output. The resonance wavelength is observed using the monitor which is placed at the sensor output. The total size of our sensor is $18\mu m \times 12\mu m$.

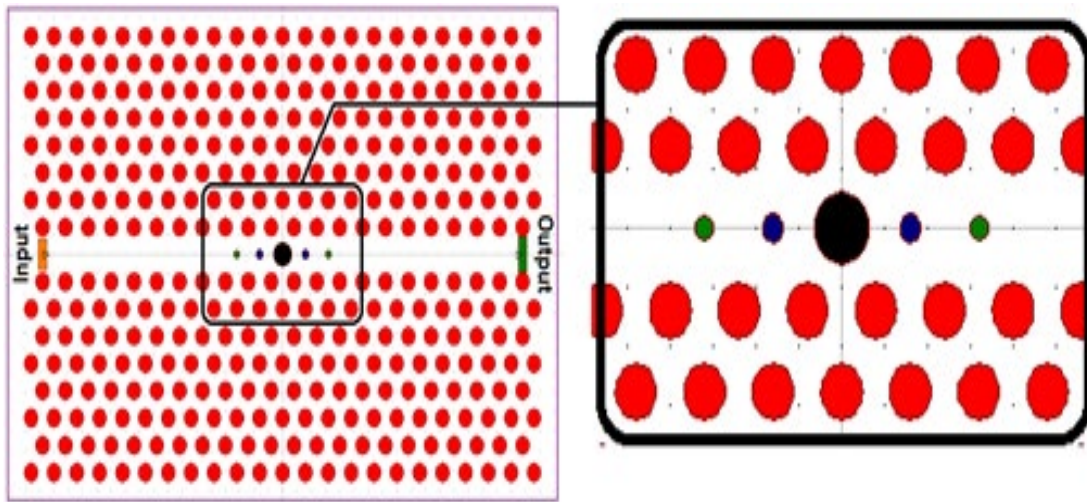


FIG. 2. Proposed design for the temperature sensor.

This section describes the optical detection results obtained for the proposed sensor structure. **FIG. 3** shows the electric field distribution of the resonant cavity for the wavelength 1682.1 nm at the output of our proposed device in the temperature range of $0^\circ C$ to $500^\circ C$ with a $50^\circ C$ step size. **FIG. 4** graphically represents the normalized transmission at the output of the proposed sensor at a zero temperature ($0^\circ C$) which corresponds to an intensity of 81.5% at the wavelength 1682.1 nm. On the other hand, the relationship of resonance wavelengths as a function of temperature has been illustrated in **FIG. 5** and recapitulated in the **TABLE 1**. The necessary functional parameters of our designed temperature sensor are compared with the already mentioned sensors, which are summarized in **TABLE 2**. It indicates that the dynamic range, quality factor ($Q = \lambda_0 / \Delta\lambda$), and sensitivity of the proposed temperature sensor are better than those of the previously existing sensor [28-34]. These results are obtained by using the Q-Finder model in RSoft software which is combined by the 2D-FDTD method with fast harmonic analysis to calculate the quality factor Q [35,36].

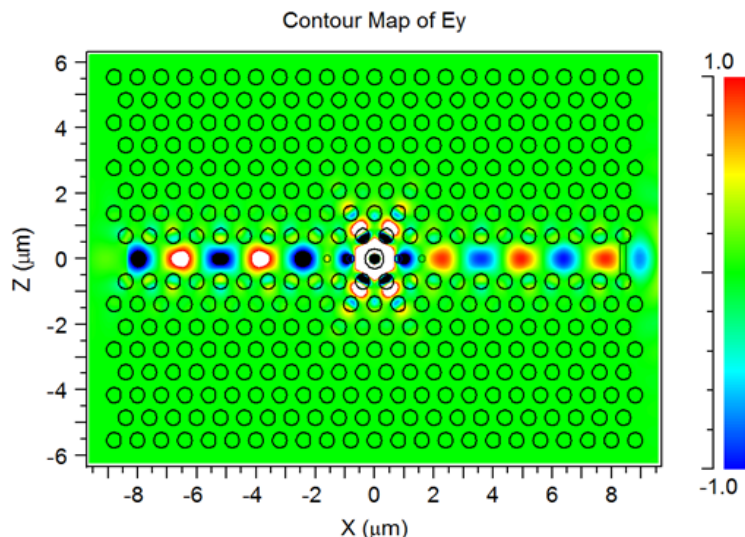


FIG. 3. Electric field distribution of resonant cavity at 1682.1 nm.

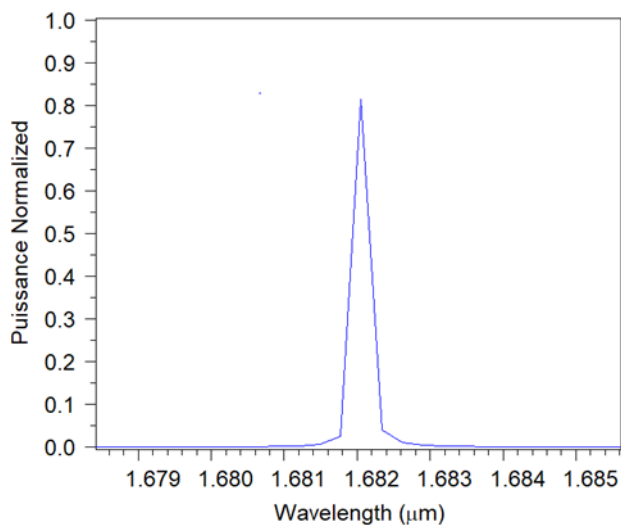


FIG. 4. Resonant wavelength of a resonant cavity at 0°C.

TABLE 1. Functional parameters for the temperature sensor at different temperature levels.

Temperature (°C)	Refractive index (RIU)	Resonance wavelength (nm)	Transmission efficiency (%)	Quality factor	Wavelength shift
0	3.42	1682.1	81.5	17 156	/
50	3.432	1687.5	62	14 688	5.4 nm
100	3.444	1693.2	64.6	12 525	5.7 nm
150	3.456	1698.6	89.6	10 943	5.4 nm
200	3.468	1704.1	92.2	10 182	5.5 nm
250	3.48	1709.7	66.7	10 412	5.6 nm

300	3.492	1714.9	96.8	11 707	5.2 nm
350	3.504	1720.6	98	14 027	5.7 nm
400	3.516	1725.9	50.8	17 234	5.3 nm
450	3.528	1731.6	53	21 105	5.7 nm
500	3.54	1737	50.1	25 349	5.4 nm

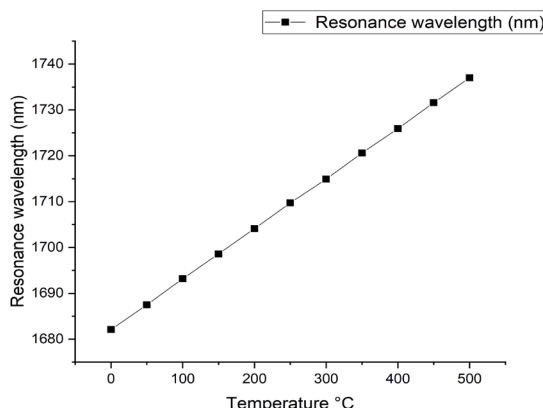


FIG. 5. The linear relation between resonant wavelengths and temperature.

TABLE 2. The proposed functional parameters of the temperature sensor compared with the previous works.

Reference	Dynamic Range (°C)	Quality factor	Temperature sensitivity (pm/°C)
Present work	0 to 500	17 156	109.8
[27]	0 to 100	/	6.6
[29]	25 to 200	214	/
[30]	0 to 450	738.7	59.25
[31]	0 to 80	2506.5	93.61
[32]	20 to 90	/	84
[33]	20 to 70	415.7	88.7
[34]	0 to 360	/	92.3

Conclusion

In this paper, we presented a two-dimensional hexagonal structure based on the resonant cavity designed for temperature sensing applications. The presence of the thermo-optical effect of the ‘Si’ material plays a very important role in the all-optical temperature sensor. The results of the PWE simulation show that the resonance frequency is shifted to a lower frequency by increasing the temperature. The study of all the functional characteristics of our proposed sensor is realized by using the PWE and FDTD methods. For temperature detection, the resonant cavity structure has a maximum quality factor of 17,156, a very high sensitivity of about 109.8 pm/°C, a dynamic range is 0°C to 500°C, and a size of $26\mu m^2$. It is therefore a design that is simple, stable, and

suitable for various applications in integrated optics.

Acknowledgement

This work was supported by the Directorate General for Scientific Research and Technological Development (DGRSDT).

REFERENCES

1. Joannopoulos JD, Johnson SG, Winn JN, et al. Molding the flow of light. Princeton Univ. 2008.
2. Ouahab I and Naoum R. A novel all-optical 4×2 encoder switch based on photonic crystal ring resonators. *Optik*. 2016;127(19):7835-41.
3. Kouddad E and Naoum R. Optimization of an all-optical photonic crystal NOT logic gate using switch based on nonlinear Kerr effect and ring resonator. *Sensor Letters*. 2020;18(2):89-94.
4. Elhachemi K and Rafah N. A novel proposal based on 2D linear resonant cavity photonic crystals for all-optical NOT, XOR and XNOR logic gates. *Journal of Optical Communications*. 2020.
5. Elhachemi K, Naoum R, Vigneswaran D et al. Performance evaluation of all-optical NOT, XOR, NOR, and XNOR logic gates based on 2D nonlinear resonant cavity photonic crystals. *Optical and Quantum Electronics*. 2021;53(12):1-5.
6. Elhachemi K, Vigneswaran D, Rafah N et al. All-optical logic gates function by ring resonator properties aiding photonic crystal. *Physica Scripta*. 2022;97(10):105502.
7. Biswas U, Rakshit JK, Das J et al. Design of an ultra-compact and highly-sensitive temperature sensor using photonic crystal based single micro-ring resonator and cascaded micro-ring resonator. *Silicon*. 2021;13(3):885-92. [Googlescholar] [Crossref]
8. Radhouene M, Chhipa MK, Najjar M et al. Novel design of ring resonator based temperature sensor using photonics technology. *photonic sensors*. 2017;7(4):311-6.
9. Wang HZ, Zhou WM, Zheng JP. A 2D rods-in-air square-lattice photonic crystal optical switch. *Optik*. 2010;121(21):1988-93.
10. Radhouene M, Monia N, Janyani V. Tunable photonic crystal switch based on ring resonators with improved crosstalk and Q-factor. *International Conference on Optical and Photonics Engineering* 2017;10250:197-201).
11. Chhipa MK, Radhouene M, Robinson S et al. Improved dropping efficiency in two-dimensional photonic crystal-based channel drop filter for coarse wavelength division multiplexing application. *Optical Engineering*. 2017;56(1):015107
12. Suthar B. Tuning of guided mode in two dimensional chalcogenide based photonic crystal waveguide. *Optik*. 2015;126(22):3429-31.

13. Park I, Lee HS, Kim HJ et al. Photonic crystal power-splitter based on directional coupling. *Optics Express*. 2004;12(15):3599-604.
14. Robinson S, Dhanlaksmi N. Photonic crystal based biosensor for the detection of glucose concentration in urine. *Photonic Sensors*. 2017 Mar;7(1):11-9.
15. Robinson S, Dhanlaksmi N. Photonic crystal based biosensor for the detection of glucose concentration in urine. *Photonic Sensors*. 2017;7(1):11-9.
16. Qian X, Zhao Y, Zhang YN et al.. Theoretical research of gas sensing method based on photonic crystal cavity and fiber loop ring-down technique. *Sensors and Actuators B: Chemical*. 2016;228:665-72.
17. Zhao Y, Zhang YN, Lv RQ et al. Electric field sensor based on photonic crystal cavity with liquid crystal infiltration. *Journal of Lightwave Technology*. 2017;35(16):3440-6.
18. Tinker MT, Lee JB. Thermal and optical simulation of a photonic crystal light modulator based on the thermo-optic shift of the cut-off frequency. *Optics express*. 2005;13(18):7174-88.
19. Zhang Y, Huang J, Lan X et al. Simultaneous measurement of temperature and pressure with cascaded extrinsic Fabry–Perot interferometer and intrinsic Fabry–Perot interferometer sensors. *Optical Engineering*. 2014;53(6):067101.
20. Wu C, Zhang Y, Guan BO. Pressure and temperature discrimination based on dual-FBG written in microstructured fiber and standard fiber. In 21st International Conference on Optical Fiber Sensors 2011;7753:1357-1360.
21. Anuszkiewicz A, Statkiewicz-Barabach G, Borsukowski T et al. F. Sensing characteristics of the rocking filters in microstructured fibers optimized for hydrostatic pressure measurements. *Optics Express*. 2012;20(21):23320-30.
22. Xu H, Hafezi M, Fan J et al. Ultra-sensitive chip-based photonic temperature sensor using ring resonator structures. *Optics Express*. 2014;22(3):3098-104.
23. Kolli VR, Talabattula S. High Q Photonic Crystal Based Microring Resonator Biosensor for the Detection of Glucose-Concentration in Urine and Blood. *International Conference on Electronics*. 2020;4(30):702-6.
24. Goyal AK, Pal S. Design and simulation of high sensitive photonic crystal waveguide sensor. *Optik*. 2015;126(2):240-3..
25. Huang L, Tian H, Yang D et al. Optimization of figure of merit in label-free biochemical sensors by designing a ring defect coupled resonator. *Optics Communications*. 2014;332:42-9
26. Jindal S, Sobti S, Kumar M et al. Nanocavity-coupled photonic crystal waveguide as highly sensitive platform for cancer detection. *IEEE Sensors Journal*. 2016;16(10):3705-10
27. Fu HW, Zhao H, Qiao XG et al. Study on a novel photonic crystal temperature sensor. *Optoelectronics Letters*. 2011;7(6):419-22.

28. Tinker MT, Lee JB. Thermal and optical simulation of a photonic crystal light modulator based on the thermo-optic shift of the cut-off frequency. *Optics express*. 2005;13(18):7174-88.
29. Boruah J, Kalra Y, Sinha RK. Demonstration of temperature resilient properties of 2D silicon carbide photonic crystal structures and cavity modes. *Optik*. 2014;125(5):1663-6.
30. Rajasekar R, Robinson S. Nano-pressure and temperature sensor based on hexagonal photonic crystal ring resonator. *Plasmonics*. 2019;14(1):3-15.
31. Bounaas F, Labbani A. Optimized Cancer Cells Sensor Based on 1D Photonic Crystal Vertical Slot Structure. *Progress In Electromagnetics Research C*. 2021;117:239-49.
32. Hocini A, Harhouz A. Modeling and analysis of the temperature sensitivity in two-dimensional photonic crystal microcavity. *Journal of Nanophotonics*. 2016;10(1):016007.
33. Chen YH, Shi WH, Feng L et al. Study on simultaneous sensing of gas concentration and temperature in one-dimensional photonic crystal. *Superlattices and Microstructures*. 2019;131:53-8.
34. Zegadi R, Ziet L, Zegadi A. Design of high sensitive temperature sensor based on two-dimensional photonic crystal. *Silicon*. 2020;12(9):2133-9.
35. Kouddad E, Naoum R. Optimization of an all-optical photonic crystal NOT logic gate using switch based on nonlinear Kerr effect and ring resonator. *Sensor Letters*. 2020;18(2):89-94.
36. Harhouz A, Hocini A. Design of high-sensitive biosensor based on cavity-waveguides coupling in 2D photonic crystal. *Journal of Electromagnetic Waves and Applications*. 2015;29(5):659-67.